Energetics of bcc-fcc lattice deformation in iron

Genrich L. Krasko* and G. B. Olson†
Department of Materials Science and Engineering, Massachusetts Institute of Technology, Cambridge, Massachusetts 02139
(Received 26 June 1989)

The energetics of homogeneous bcc-fcc lattice deformation in iron at 0 K has been investigated along the tetragonal "Bain" deformation path. The total energy (as a function of volume), the enthalpy (as a function of pressure), the pressure-volume relations—both for nonmagnetic (NM) and ferromagnetic (FM) states—were calculated using the linear muffin-tin-orbital (LMTO) method. The ground-state magnetic properties (ferromagnetic contributions to the total energy and magnetic moments) were found by making use of the Stoner theory of itinerant ferromagnetism, rather than spin-polarized calculations. This circumvents the difficulties of using the traditional local-spin-density approximation which fails to describe correctly the energetics of iron phases. The Stoner exchange parameter I was calculated from the linear-response theory for each axial ratio c/a as a function of volume and then adjusted by a constant enhancement factor β, determined by fitting the equilibrium atomic volume of the FM bcc phase. No other adjustments of any quantities were performed. The calculations revealed a somewhat unusual behavior of enthalpy along the deformation path. The enthalpy of the NM phase exhibits a monotonic decrease with c/a, the bcc modification being unstable with respect to the shear deformation. Moreover, up to a certain c/a (depending on pressure), the NM bcc phase is also unstable with respect to spontaneous magnetization. Ferromagnetism stabilizes the bcc phase. However, the FM fcc phase is unstable with respect to shear deformation. The enthalphy curve along the deformation path then has a cusp corresponding to a first-order phase transition between FM and NM states accompanied by an appreciable volume discontinuity. For the FM bcc, the calculated bulk modulus (1.689 mbar) and the magnetic moment ($2.223\mu_B$/atom) as well as the fcc-bcc enthalpy difference at zero pressure (6.947 kJ/mol) are in good agreement with available experimental data. A fcc-bcc lattice-deformation enthalpy barrier at the equilibrium pressure $P_0=145$ kbar is found to be 12.762 kJ/mol. The NM fcc lattice loses mechanical stability at a fcc-bcc enthalpy difference of -14.072 kJ/mol. As an aid to the development of improved interatomic potentials for iron, plots of FM contributions to the energy versus Wigner-Seitz radius for different c/a are also presented.

I. INTRODUCTION

The bcc-fcc phase transformation in iron lies at the core of the unique properties of iron-base materials. This transformations, being a typical representative of the family of martensitic transformations (MT's), has been studied for decades (for references see, e.g., Refs. 1-3). Unlike most of the polymorphic transformations in solids, the MT is a diffusionless process involving a correlated motion of many atoms. One important aspect of such motion is the energetics of large-strain homogeneous lattice deformation. This contributes a local energy density of importance to interfacial energy and mobility as well as the energetics of potential nonclassical nucleation mechanisms.[1] The homogeneous deformation describes a continuous crystallographic transition from initial to final phase. In the case of the bcc-fcc MT a few homogeneous strain paths have been suggested (see, e.g., Ref. 3). The simplest one, known as the Bain deformation,[4] consists of a continuous expansion of a bcc lattice along one of the cubic axes with a contraction along the two others. When the c/a ratio reaches the value $\sqrt{2}$, the body-centered-tetragonal lattice (bct) just becomes fcc (see Fig. 1). More complex "two-strain" paths are realized in bcc-hcp martensitic transformations.[5] It can also be true for iron.[6] However, the Bain path is unique in that it retains the highest crystal symmetry. Pseudopotential calculations for the bcc-fcc lattice deformation in Na have shown this path to have the lowest energy barrier on the class of orthorombic deformations.[7] From these considerations, the Bain path is a convenient tool for investigating the energetics of the transformation. In the past, it has been used in both phenomenological and *ab initio* calculations of the energetics of MT.[8]

Along the deformation path $1\le c/a\le\sqrt{2}$, one obviously expects the total energy (or the enthalpy in the constant-pressure regime) to undergo a maximum. The nature of this maximum in the case of iron is not clear *a priori*. At low temperatures and moderate positive pressures bcc iron is ferromagnetic (FM), while fcc iron is paramagnetic. Somewhere along the transformation path, the ferromagnetism is to disappear. One can expect that this magnetic transition plays a major role in the energetics of the martensitic transformation.

So far, no reliable information on the value of the enthalpy maximum or the enthalpy profile as a whole is

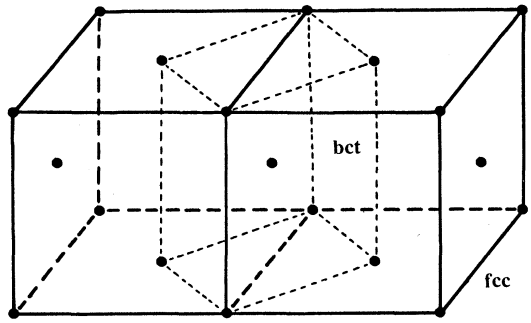

FIG. 1. The Bain correspondence between bct and fcc crystal lattices. Solid lines, fcc unit cells; dashed lines, bct cell. Not all the lattice points of fcc are shown.

available. No first-principles, microscopic calculations of the total energy (or enthalpy) of iron along the Bain path has been done thus far. Such calculations are the objective of the present work.

In recent years iron has been the object of extensive study by various first-principles methods (for references and comparison of results for iron obtained by different methods, see, e.g., Refs. 9-13). However, the self-consistent spin-polarized calculations on bcc iron inevitably failed to predict the relative stability of the FM bcc phase with respect to the nonmagnetic (NM) fcc (see discussion in Ref. 13). This failure is believed to be mainly due to the local-spin-density approximation (LSDA) used in the calculations.

Because of this fundamental difficulty, at the present time, an entirely *ab initio* analysis of the structural phase transformations in iron is not possible. An alternative approach is to introduce into the theory an adjustable parameter in order to make calculations more consistent with experimental observations.

Along this path, we have chosen to calculate the equilibrium magnetic moments as well as the magnetic contributions to the ground-state energies of iron using the Stoner model of itinerant ferromagnetism,[14] rather than performing spin-polarized calculations. The Stoner exchange parameter I can then serve as an adjustable parameter. Having made only one adjustment, such a procedure enabled us to perform the complete analysis of the energetics of the bcc-fcc lattice deformation in iron.

We used the LMTO method[15] with the so-called combined-correction term,[15] and the Madelung electrostatic correction.[16] Scalar-relativistic calculations on uniform meshes of 1540 points in the irreducible wedges of bct Brillouin zones were done, with the exchange-correlation functional of von Barth and Hedin.[17] Also, the frozen-core approximation was used.[18]

The plan of this paper is as follows. In Sec. II we discuss the Stoner model as applied to self-consistent non-spin-polarized calculations, and briefly outline the procedure of the calculations. In Sec. III, we discuss the calculations of structural properties of bcc and fcc modifications of iron. Then, in Sec. IV, the energetics and magnetic behavior of the crystal lattice along the Bain-deformation path are discussed. We show that, for a given pressure, a first-order magnetic phase transition occurs at a definite c/a ratio, resulting in a cusp on the enthalpy versus c/a plot, and a volume discontinuity. We show that the NM bcc and bct phases are (up to a certain c/a) thermodynamically unstable with respect to spontaneous magnetization. Moreover, the NM bcc phase is unstable with respect to shear along the deformation path. Another unexpected result is that, though exhibiting an interesting metamagnetic behavior, the FM fcc phase also cannot exist: it is unstable with respect to the shear deformation.

II. STONER MODEL OF ITINERANT FERROMAGNETISM AND PROCEDURE OF CALCULATIONS

The Stoner theory, first suggested in 1939,[14] has been successfully used in recent years in estimating both the equilibrium magnetization and magnetic energy of band electrons. This was made possible as a result of a rigorous formulation of the Stoner model as a perturbation approach in terms of microscopic electronic theory.[19–22] Particularly, the fundamental parameter of the theory, the Stoner exchange parameter I, was understood in terms of density-functional characteristics. In iron, the theory explained the metamagnetic behavior of the fcc phase.[19,23] Recently, some more light has been shed on the metamagnetic behavior of fcc iron.[24] The Stoner approach in combination with self-consistent non-spin-polarized calculations enables one to perform the detailed analysis of FM behavior as well as identify all the possible magnetic stationary phases, stable, metastable, and even unstable, and find the areas of their emergence. Such an analysis, using traditional spin-polarized calculations is at present either too cumbersome and computationally expensive or even impossible.[25]

The Stoner model in its original formulation postulates that the change of energy upon forming a FM state with moment $\mathbf{m}$ consists of two parts. The exchange energy contribution is simply $-\frac{1}{4}I\mathbf{m}^2$, where the exchange parameter I is a constant. The kinetic-energy term is found by forming two subbands for spin-up and spin-down electrons by flipping $\mathbf{m}/2$ spin-down electrons from just below the NM Fermi level into the unoccupied spin-up states just above the Fermi level. As was shown in Refs. 19–22, this procedure corresponds to the first-order perturbation theory in $\mathbf{m}/n_v$ (n_v is the number of valence electrons per atom).[29] Thus, for a given $\mathbf{m}$, the magnetic contribution to the total energy is

$$E_m=\tfrac{1}{2}\int_0^{\mathbf{m}}\frac{\mathbf{m}'}{\overline{N(\mathbf{m}')}}d\mathbf{m}'-\tfrac{1}{4}I\mathbf{m}^2\,, \tag{1}$$

where $\overline{N(\mathbf{m})}$ is the NM density of states averaged between the Fermi levels of spin-up and spin-down electrons as found from the rigid-subband shift. The procedure of "constructing" $\overline{N(\mathbf{m})}$ is described elsewhere (see, e.g., Ref. 15).

The stationarity requirement, $\partial E_m/\partial\mathbf{m}=0$, gives,

apart from the "trivial" solution, $\mathbf{m}=0$, the criterion of an emerging FM state:

$$I\overline{N(\mathbf{m})}=1 \ . \tag{2}$$

Suppose Eq. (2) has a solution, $\mathbf{m}$. Then, the corresponding FM state is stable ($\partial^2 E_m/\partial \mathbf{m}^2>0$) if

$$\partial\overline{N(\mathbf{m})}/\partial \mathbf{m}<0 \ ; \tag{3}$$

otherwise it is unstable ($\partial^2 E_m/\partial \mathbf{m}^2<0$). However, even if Eqs. (2) and (3) hold, the FM state may not occur if $E_m>0$. In this case the FM state is metastable.

As for the NM state, $\mathbf{m}=0$, it is stable and may coexist with a FM state (metamagnetic situation), only so far as

$$(\partial^2 E_m/\partial \mathbf{m}^2)_{\mathbf{m}=0}>0 \tag{4}$$

or, equivalently,

$$I\overline{N(E_F)}<1 \ , \tag{5}$$

where $\overline{N(E_F)}$ is the NM density of states (DOS) at the Fermi level [$\overline{N(E_F)}=\overline{N(0)}$].

From the perturbation-theory analysis,[19–22] I can be found in terms of the NM system. From the linear-response theory[22] it follows that

$$I=\int d^3r\, \gamma^2(r)|K(r)| \ , \tag{6}$$

where

$$\gamma(r)=\sum^{\text{occ}} \frac{\delta(E_F-E_i)|\psi_i(r)|^2}{N(E_F)} \ ,$$

and

$$K(r)=\tfrac{1}{2}[d^2E_{\text{xc}}(r,\mathbf{m})/d\mathbf{m}^2]_{\mathbf{m}=0} \ .$$

Here E_i and $\psi_i(r)$ are, respectively, the eigenvalues and the wave functions of the NM system; $E_{\text{xc}}(r,\mathbf{m})$ is the exchange-correlation functional.

Until recently, the Stoner parameter I has been believed to be essentially a constant, independent of both the volume and the crystal structure of the metal. Our calculations for both fcc and bcc (Refs. 24 and 30) revealed the monotonic behavior of I as a function of the Wigner-Seitz (WS) radius, s. The magnetic energy, Eq. (1), the equilibrium magnetic moment, $\mathbf{m}$ [as found from Eq. (2)], and the equilibrium atomic volume happen to be rather sensitive to the values of I. The idea of this paper (as well as Ref. 30) is to adjust the value of I, so that the equilibrium WS radius, s_0, for the FM bcc phase is equal to the experimental value. In Table I we compare the calculated s_0 for $I=\beta I_0$ [where I_0 is the *"ab initio"* value, Eq. (6), and $\beta=1.000$, 1.025, 1.050, 1.075, and 1.090]. One can see that for $\beta=1.075$ the equilibrium WS radius, $s_0=2.659$ a.u., almost matches the experimental value. Therefore, we have chosen $\beta=1.075$ as the "universal" enhancement factor; all the calculations for the whole range of c/a values were done with this β.[31] No other adjustments of any parameters were performed.

Our calculations were done for 17 c/a values: $0.92\le c/a\le 1.46$. For each c/a, self-consistent non-spin-polarized calculations were performed for nine values of the WS radius, s ($2.521\le s\le 2.788$ a.u.). In each calculation, after convergence had been achieved, the Stoner parameters $I_0(c/a,s)$, Eq. (6), and then $I=1.075I_0$ were found and the averaged DOS, $\overline{N(\mathbf{m})}$, was generated. Then the Stoner equation, Eq. (2), was solved for the equilibrium magnetic moment, $\mathbf{m}$, and the magnetic energy E_m was calculated from Eq. (1). In a metamagnetic situation, all the stable magnetic solutions were identified.

TABLE I. Dependence of the equilibrium WS radius for the FM bcc phase on the Stoner-parameter enhancement factor β.

β	s (a.u.) (2.661)[a]
1.000	2.648
1.025	2.650
1.050	2.654
1.075	2.659
1.090	2.664

[a]Experimental value, Ref. 34.

In the next step, the total energy (consisting of the nonmagnetic, magnetic, and electrostatic contributions) was approximated (with rms$\approx$0.03 mRy) by the six-term function[32]

$$E(c/a,s)=E_1+E_2/\Omega^{2/3}+E_3/\Omega^{4/3}+E_4/\Omega^{6/3}+E_5/\Omega^{8/3}+E_6/\Omega^{10/3} \ .$$

The pressure P and the bulk modulus B were then found by analytic differentiation with respect to the atomic volume Ω.

We believe that the proposed procedure of using the Stoner model may be extremely useful in studies of iron-based systems. Not only does it allow one to make the calculations faster and cheaper, it enables one to perform analysis beyond the ability of traditional spin-polarized calculations: The phase instabilities we will discuss subsequently simply could not be found by the traditional approach.

III. STRUCTURAL PROPERTIES OF bcc AND fcc PHASES

We first will summarize the results for the bcc and fcc phases of iron (see also Ref. 30). In Table II we compare the calculated magnetic moment $\mathbf{m}(s_0)$ and the bulk modulus $B(s_0)$ for the bcc and fcc phases as well as the bcc-fcc energy difference at absolute zero with the corresponding experimental values. One can see that the single adjustment resulted in good matches between calculated and experimental values for the most important structural properties. The negative energy difference is very close to the experimental value. Also, there is excellent agreement for the bulk modulus of FM bcc phase.

From the physical point of view, the enhancement of I (and thus the enhancement of spin-spin correlation, known to be underestimated in the LSDA's) simply led to an expansion of the FM lattice with the corresponding

TABLE II. Comparison of calculated and experimental structural properties of bcc and fcc iron.

	FM bcc		NM fcc		FM fcc[a]		$E_{\text{NM-fcc}}-E_{\text{FM-bcc}}$ MRy/atom (kJ/mol)	
	Calc.	Expt.	Calc.	Expt.	Calc.	Expt.	Calc.	Expt.
s_0 (a.u.)	2.659	2.661[b]	2.588	2.62[c]	2.690	2.68[d]		
B (mbar)	1.689	1.67[e]	3.122		2.317		5.307	4.166[g]
m (μ_B/atom)	2.223	2.15[f]			2.595	2.4−2.8[d]	(6.947)	(5.456)
								3.692[h]
								(4.833)

[a]High spin (HS).
[b]Reference 34.
[c]Empirical calc., Ref. 33.
[d]Two-spin model, Ref. 33.
[e]Reference 35.
[f]Reference 9.
[g]Reference 33.
[h]Reference 36.

favorable shifts in the magnetic energy and the bulk modulus.

The adjustment of the exchange interaction, however, does not eliminate the drawbacks of the LSDA for NM phases. The equilibrium WS radius for the metastable NM fcc phase, $s_0=2.588$ a.u., is shifted too far away from that of the FM bcc phase (2.661 a.u.). One can see from Table II and Fig. 2 that the relative change of equilibrium volumes is about 9%, while the empirical estimates based on experimental data give only 5%.[33] The bulk modulus is probably also too high.

Figure 2 shows the plots of the total energies versus s for the NM and FM phases of both the bcc and fcc iron. In Ref. 24 the metamagnetic behavior of fcc iron was discussed in detail. Here we shall focus primarily on the bcc phase (the fcc curves are virtually the same as in Fig. 5 of Ref. 24).

As one can see, the FM phase in bcc iron has the lowest energy. The NM bcc phase was always believed to be metastable—i.e., having a higher energy, but corre-

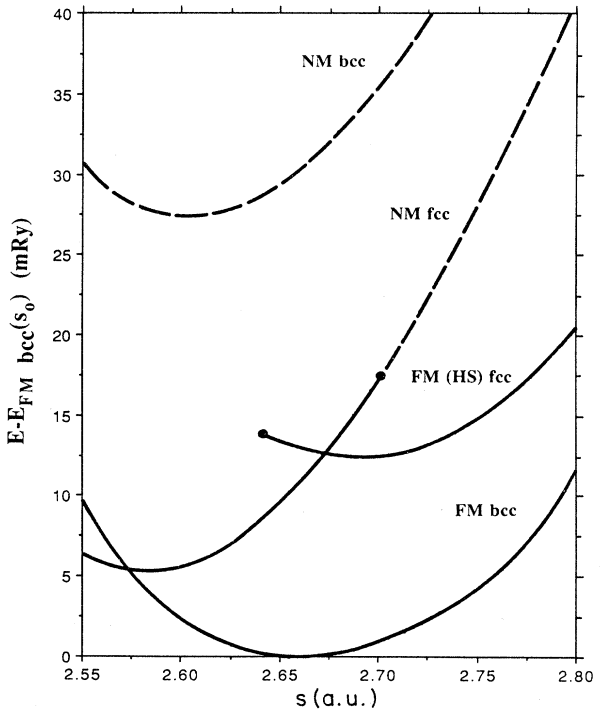

FIG. 2. The total energies of fcc and bcc phases of iron vs WS radius s. For the FM fcc phase only the energy of the HS states is shown (see also Fig. 5). The dashed lines correspond to the states unstable with respect to spontaneous magnetization. The solid dots here and in other figures show the borders of stability.

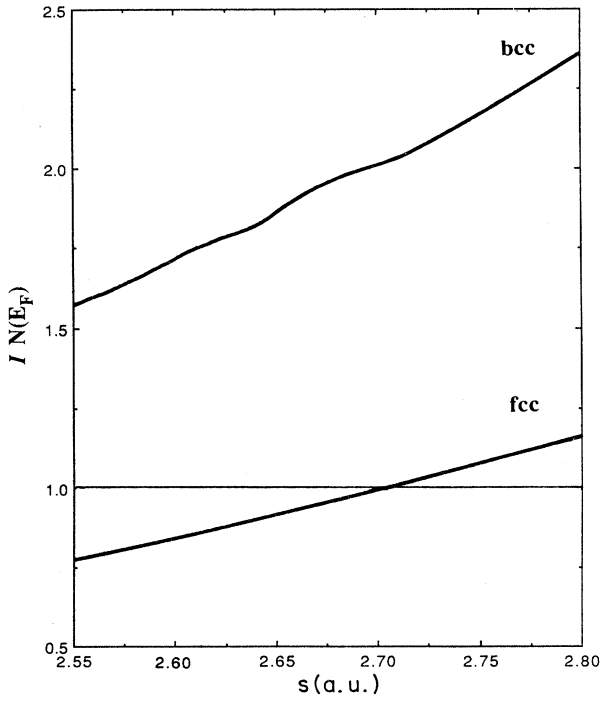

FIG. 3. The parameter $IN(E_F)$ as a function of the WS radius s. A nonmagnetic phase is unstable with respect to spontaneous magnetization if $IN(E_F)>1$. $IN(E_F)=1$ for the fcc phase corresponds to the point in Fig. 2 where the NM fcc phase becomes unstable (dashed line starts).

sponding to a local energy minimum. However, the unexpected significant result is that the NM bcc phase is unstable with respect to spontaneous magnetization for all volumes considered.

It follows from Eq. (5) that the NM phase is stable only so far as $IN(E_F)<1$. However, $N(E_F)$ in bcc iron is too high for Eq. (5) to hold. Figure 3 shows $IN(E_F)$ versus s.[37] This result demonstrates the importance of distinguishing a "paramagnetic" phase from a "nonmagnetic" one. This has been stressed in the literature (see, e.g., Refs. 9 and 38). Our point is that the nonmagnetic phase in iron is not a good model for the paramagnetic phase: the former is simply unstable. The Curie temperature where the ferromagnetism disappears (1043 K in iron) corresponds to the disappearance of the long-range magnetic order, not the spin polarization itself. The latter, in the Stoner theory which neglects the local magnetic order, disappears in iron only around 4000–6000 K;[21] i.e., the local magnetic moments persist in bcc iron up to the melting point.

Figure 4 shows the magnetic moments versus s. Note, the plot for the bcc phase exhibits a "bump" in the vicinity of s_0 (2.661 a.u.). This same feature, though much less pronounced, can also be seen in Fig. 6 of Ref. 27.

The magnetic contributions to the total energies found

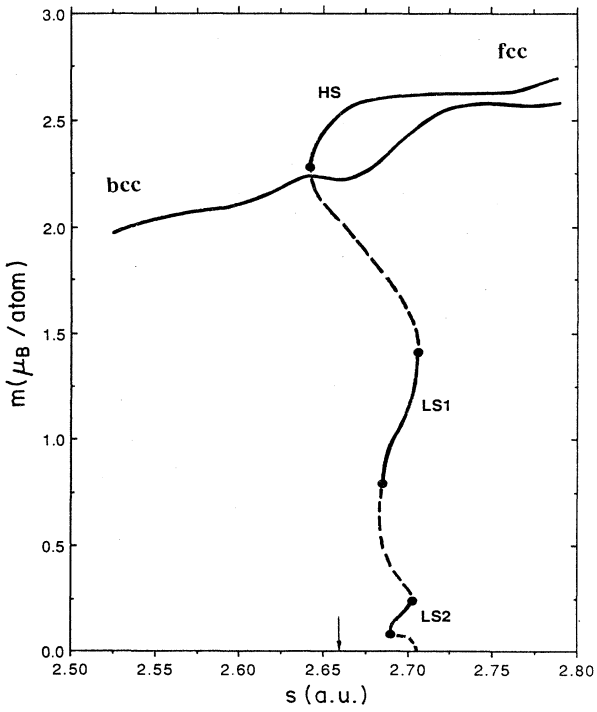

FIG. 4. Stationary magnetic moments as a function of the WS radius. The plot for the bcc phase has a pronounced "bump" around $s=s_0$ (shown by an arrow). The dashed parts on the fcc curve correspond to the magnetic states which are unstable ($\partial^2 E_m/\partial m^2<0$). The fcc plot is virtually the same as Fig. 4 of Ref. 24.

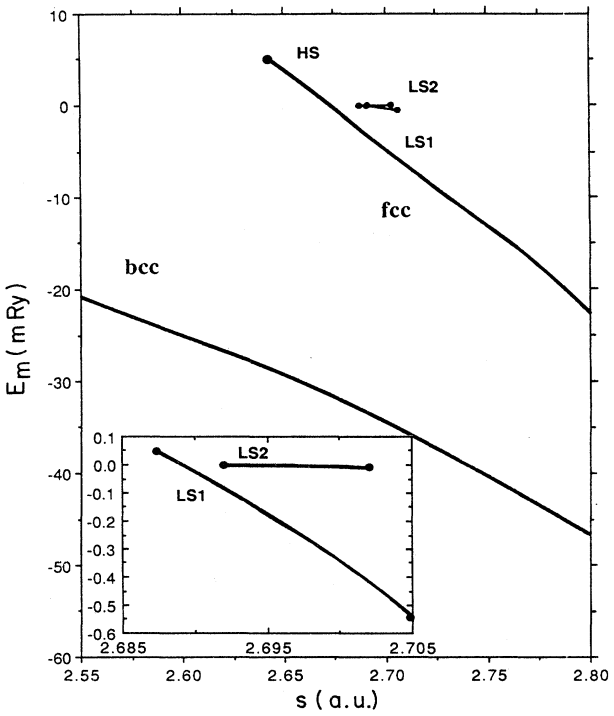

FIG. 5. Magnetic energy E_m of fcc and bcc phases. Note that the three ferromagnetic fcc phases have regions of metastability ($E_m>0$). An expanded plot is shown for the two LS phases.

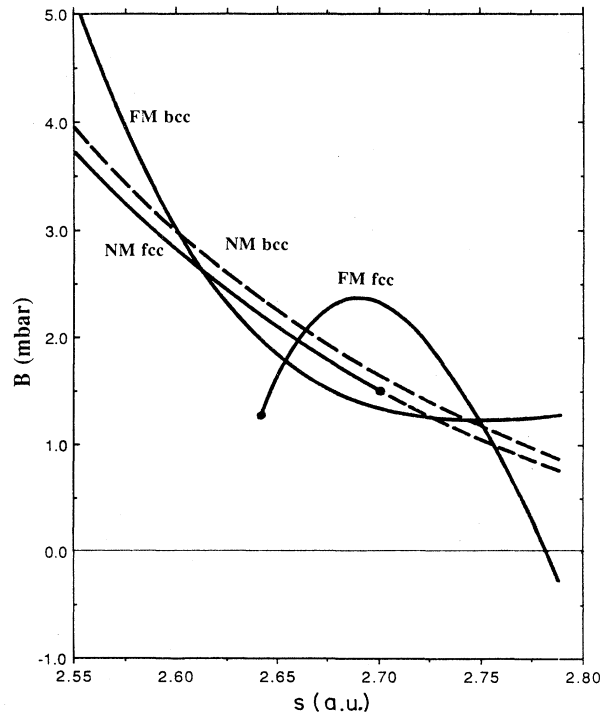

FIG. 6. Bulk moduli vs s. As in the previous figures, the dashed lines indicate the unstable nonmagnetic states.

from Eq. (1) are shown in Fig. 5. The fcc phase is metamagnetic: In a constant-volume regime there are three stable ferromagnetic phases:[24] high-spin (HS) and two low-spin (LS1 and LS2) phases. The LS phases have high volume and would correspond to very high negative pressures.

The plots in Fig. 5 look quite smooth, though, in fact, both the fcc and bcc magnetic energies undergo changes of their second derivatives with respect to volume. As one can see from Fig. 6, the bulk modulus of the FM fcc phase has a maximum at $s=2.690$ a.u., followed by a volumetric instability ($B<0$) at $s=2.782$ a.u. The behavior of the FM bcc bulk modulus is also somewhat unusual. One could have expected a monotonic decrease of $B(s)$. Instead, the plot demonstrates a flat minimum. Of course, at some higher lattice expansion, $B(s)$ should eventually reach zero.

Figure 7 shows the enthalpy plots. One can see that the FM bcc–NM fcc phase transformation occurs at $P=145$ kbar. Empirical calculations[33] give 150 kbar for this point. Experimentally, at 0 K, the FM bcc–NM hcp phase transition would be observed at approximately the same pressure.[33]

Figure 8 demonstrates the equations of state for the bcc and fcc phases. The experimental points[39–41] for the FM bcc phase closely follow the calculated curve, which could have been expected due to the excellent agreement of calculated and experimental bulk moduli (Table II).

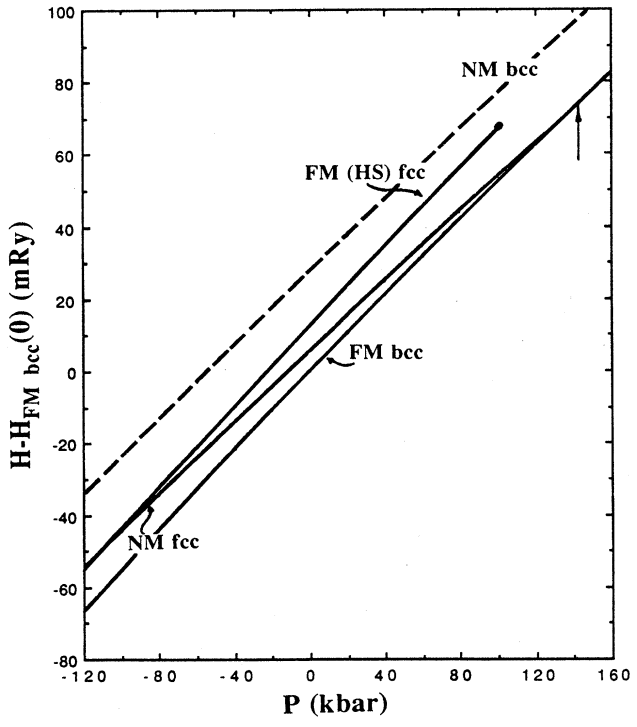

FIG. 7. Enthalpies of the bcc and fcc phases vs pressure. At $P_0=145$ kbar the FM bcc and NM fcc phases are at equilibrium (an arrow on the plot).

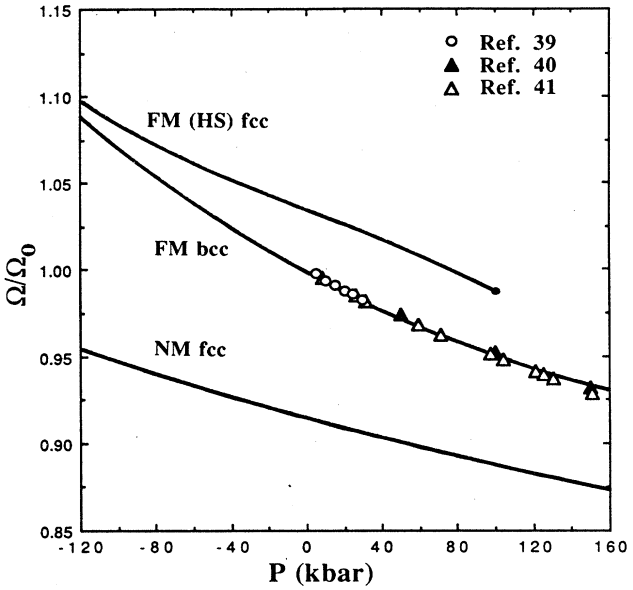

FIG. 8. The equations of state for the iron phases. Ω_0 is the atomic volume of the FM bcc phase at $P=0$.

The plot for FM fcc of course reflects the peculiarity of the behavior of the bulk modulus. Unfortunately, as we pointed out in the Introduction, all the detailed calculated information on the FM fcc phase is not of much physical relevance since the latter is unstable with respect to tetragonal shear deformation. These observations will be discussed in the next section.

IV. BEHAVIOR ALONG THE BAIN PATH

From an intuitive point of view one could expect that upon imposing a uniform deformation, the enthalpy plots of both NM and FM phases would have double-well shapes with minima at the bcc and fcc states and an intermediate smooth maximum at $1\leq c/a\leq\sqrt{2}$. Such a picture was observed in sodium[7,8] and recently in copper.[42]

Figure 9 shows results of our previous pseudopotential calculations[7] for the bcc-fcc Bain deformation in Na. Smooth curvess were obtained over the range $P=-15.4$–200 kbar including the equilibrium pressure $P_0=87.6$ kbar.

Unexpectedly, for iron, the calculated picture is quite different. Figure 10 shows our results for three pressures: 140, 0, and −120 kbar. At 140 kbar the FM bcc and NM fcc phases are almost at equilibrium (the exact equilibrium takes place at $P_0=145$ kbar, as one can see in Fig. 7). Though we already know that the NM bcc phase is unstable with respect to spontaneous magnetization, we still could expect that, disregarding the magnetic instability, it should correspond to a local enthalpy minimum along the c/a path. Instead, at all pressures, the NM bcc enthalpies have a maximum: e.g., the NM bcc phase is also unstable with respect to tetragonal (shear) deforma-

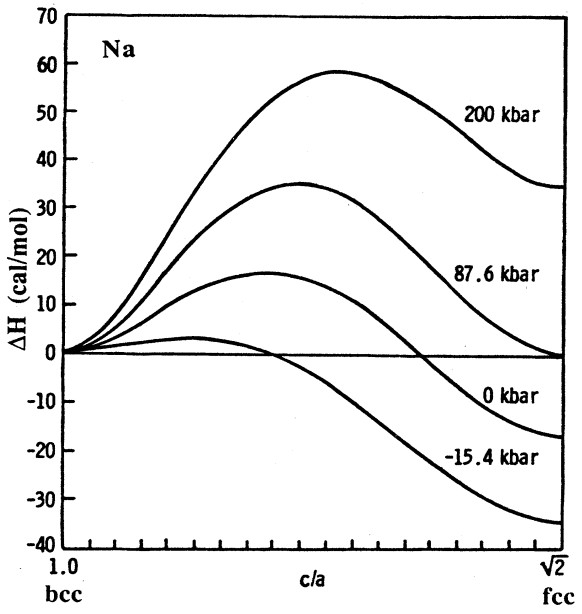

FIG. 9. Enthalpy plots along the Bain-deformation path for Na calculated using the pseudopotential method (Ref. 7).

tion. The FM contribution stabilizes the bct phases near the bcc one with an enthalpy minimum at $c/a=1$. However, at high pressures, approaching the fcc region, ferromagnetism disappears and the FM solution does not correspond to an extremum (either a minimum or a maximum) of energy (or enthalpy). At lower pressures, however, where the FM solution does exist, the FM fcc phase corresponds to an enthalpy maximum. This simply means that the FM fcc phase is unstable with respect to tetragonal deformation, and therefore cannot exist.

This is an important new result. In the past, in order to explain the thermodynamics of fcc iron, a two-spin model was postulated.[33,43] It was proposed that a mixture of two magnetic states—high-spin FM and low-spin antiferromagnetic (AFM) states—could exist in fcc iron. We have found, however, that a homogeneous FM state in fcc iron is unstable. An AFM state can exist and has been observed experimentally at low temperatures.[44] As for the FM fcc phase, it has been observed as precipitates in Cu-Au alloys,[45] and thin fcc films grown epitaxially on Cu surfaces were reported to be FM.[46] In both cases finite-size effects could be responsible for the relative stability of the FM fcc phase.

Thus, going along the Bain path from bcc to fcc, first the FM bcc phase is stable, but near $c/a=1.2$, a first-order phase transition occurs, and at higher c/a the NM face-centered-tetragonal (fct) phase is stable. As a result, the enthalpy plot is not a smooth double-well curve, but has a cusp.

The plots shown for the three pressures have common features. The FM and NM curves are almost identical in shape for the three pressures, but shifted with respect to each other. Upon lowering the pressure, the intersection point (and the cusp) shifts to the fcc direction, allowing the FM phase to have a wider range of stability. At pressures lower than about -110 kbar, the NM fcc is no longer stable. At the fcc point one can see that with the pressure decreasing the enthalpy of the FM state goes down, becoming lower than that of the NM state, which looks like a NM-FM phase transition (Figs. 3 and 7). However, as discussed above, the FM fcc phase is unstable with respect to the tetragonal deformation. As a result, with such lattice expansion, the fcc phases (both FM and NM) cease to exist, though we do not know how an AFM phase would behave at such a negative pressure. Our calculations suggest that the fcc-phase mechanical instability (corresponding to vanishing of a shear modulus) occurs at a fcc-bcc enthalpy difference of 11.067 mRy (14.487 kJ/mol).

The FM phases have larger volumes compared to their

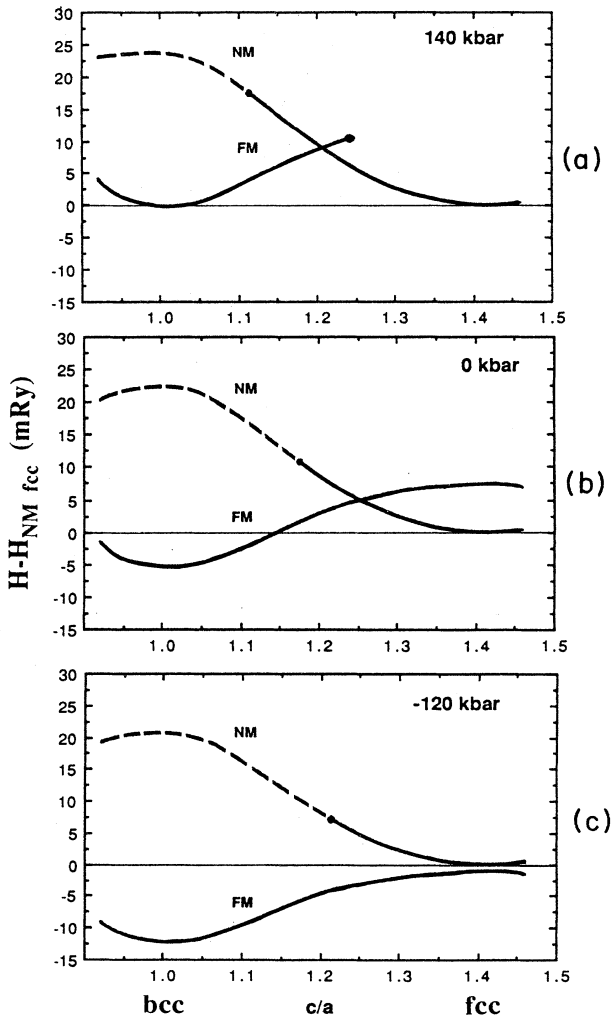

FIG. 10. The enthalpy plots along the Bain path for iron at three pressures.

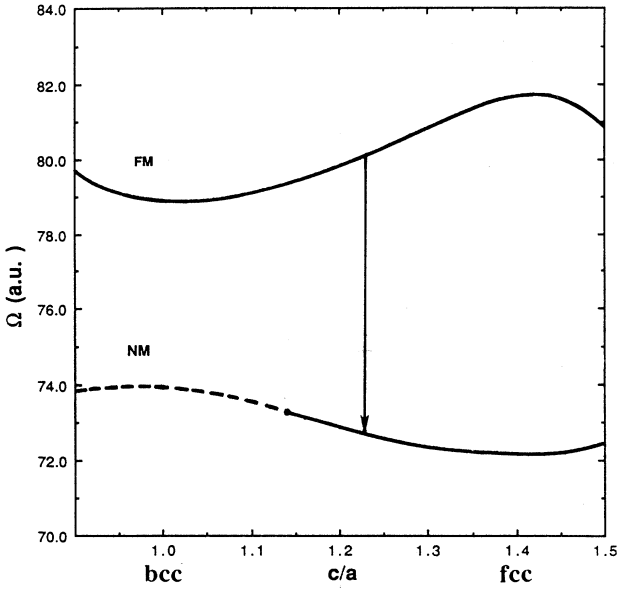

FIG. 11. Atomic volume vs c/a for $P=0$ kbar. The arrow shows the volume discontinuity at the enthalpy cusp point.

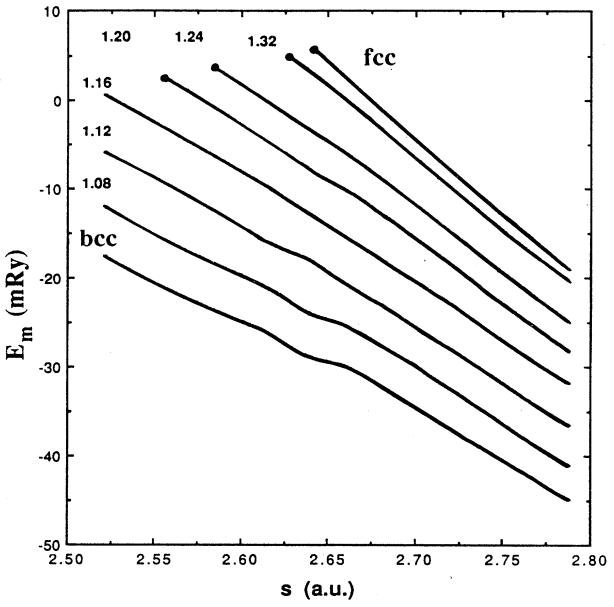

FIG. 13. Ferromagnetic contributions E_m vs s for different c/a. Solid dots indicate the points where FM phases cease to exist (do not correspond to either a minimum or a maximum of energy).

NM counterparts. Therefore, the first-order phase transitions along the Bain path are accompanied by a considerable volume discontinuity at the cusp points. Figure 11 shows the plots of atomic volume versus c/a for $P=0$ kbar. The arrow indicates the discontinuity in volume at the cusp point, which is quite large—almost 10%. Because of the volume discontinuity, the apparent cusp points from the curve intersections in Fig. 10 do not properly represent the enthalpy barrier for homogeneous lattice deformation. This can instead be determined from the saddle point of dilatation-shear energy surface. In Fig. 12 the contour plot for this surface is shown for the bcc-fcc equilibrium pressure $P_0=145$ kbar. The energy

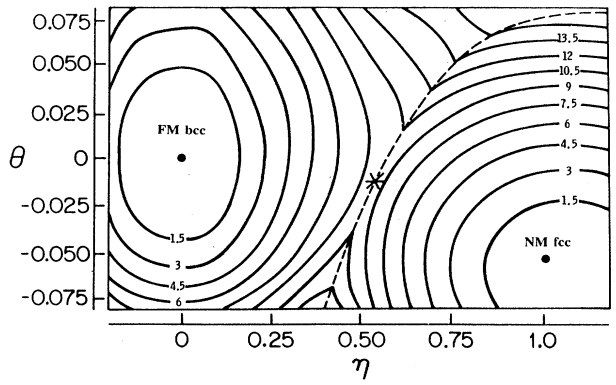

FIG. 12. Enthalpy contour plot in the dilatation-shear plane for $P_0=145$ kbar. The energy values are in mRy. Asterisk shows saddle-point deformation barrier (9.750 mRy). The coordinates are $\eta=(c/a-1)/(\sqrt{2}-1)$; $\theta=(\Omega-\Omega_0)/\Omega_0$; Ω_0 is the atomic volume of the FM bcc phase.

barrier for this case is found to be 9.750 mRy (12.762 kJ/mol).

As was mentioned above, the Stoner approach has the advantage of calculating the NM and FM contributions separately, thus defining the magnetic contribution to the deformation resistance. As an aid to the development of improved interatomic potentials for Fe, Fig. 13 plots the FM contributions to energies versus s for different c/a. This then can be added to the nonmagnetic part modeled by simple interatomic potential functions (i.e., within the embedded-atom method).

From a plot of energy versus c/a at constant volume, the elastic constants of the bcc and fcc lattices can be estimated. Along the Bain-deformation path the modulus responsible for lattice stability is $c'=\frac{1}{2}(c_{11}-c_{12})$. For FM bcc at $P=0$, the calculated $c'=0.849$ mbar is twice the experimental value, 0.475 mbar.[35] We attribute this discrepancy to the atomic-sphere approximation (ASA); more reliable values of elastic constants would be calculated if corrections for nonsphericity of the electron charge density are taken into account.[47]

V. CONCLUSIONS

Using the Stoner model with the adjusted exchange parameter, we have calculated the structural properties of bcc and fcc iron and, for the first time, the energetics of the intermediate states along the Bain-deformation path. Unexpected and somewhat unusual features of the energetics were discovered. It was found that the NM bcc phase cannot exist due to magnetic and shear instabili-

ties. Another important result is that the FM fcc phase is also unstable with respect to tetragonal deformation.

Despite some of the quantitative uncertainties remaining, these calculations clearly revealed a different class of lattice-deformation energetics compared to the simple metals previously investigated. A significant feature of the smooth curves computed for Na as depicted in Fig. 9 is that second-order elastic constants (elastic shear moduli) of a metastable lattice soften smoothly as the condition for lattice instability is approached. This is reflected in the reduced curvature around the local enthalpy minima of Fig. 9. In contrast, for Fe, the relative displacement of two enthalpy surfaces (NM and FM) of nearly constant shape defining the cusps in Fig. 10 show no such "precursor" lattice softening as the condition is approached for the abrupt loss of mechanical stability of the fcc lattice. This accounts for the relative absence of lattice-instability precursor phenomena in Fe-based alloys compared to simple alloys.[48] Further, the lattice-deformation enthalpy barrier at P_0 is found to be 2 orders of magnitude higher for Fe than for Na. This contributes to a substantially higher interfacial energy which in turn increases the critical "driving force" (bcc-fcc energy difference) for nucleation. This applies to both "classical" nucleation involving nuclei with the fully developed product phase structure and "nonclassical" nucleation involving nuclei of intermediate structure.[49–51] The latter type of nucleation is predicted to occur if transformation proceeds under conditions sufficiently close to lattice instability of the parent phase. The fcc-bcc martensitic transformation in Fe-based alloys typically nucleates at a fcc-bcc free-energy difference of -1.3 to -1.7 kJ/mol.[1–3] Based on the calculations presented here, this amounts to only 10% of the critical energy difference for fcc lattice instability, as discussed in more detail elsewhere.[51] Nonclassical nucleation is highly unlikely under these conditions.

We hope that the suggested approach will pave the way for further detailed studies of the behavior of iron and iron-based systems, including the structure and properties of martensitic interfaces.

ACKNOWLEDGMENTS

One of the authors (G.L.K.) expresses deep gratitude to Professor Ole K. Andersen and the members of his group for the hospitality extended during the author's stay at the Max-Planck-Institut für Festkörperforschung in Stuttgart, Federal Republic of Germany, where the present work was started. Many fruitful discussions with O. K. Andersen, N. Christensen, O. Gunnarsson, and O. Jepsen of the Max-Planck-Institut are gratefully acknowledged, and, especially, the invaluable help of Niels Christensen, whose linear muffin-tin-orbital code has been used in all the calculations. G. L. K. is also grateful to R. P. Adler and R. J. Harrison of the U.S. Army Materials Technology Laboratory (MTL), where the research is presently continuing, and Professor A. L. Roitburd of the University of Maryland for valuable discussions. Research at the Massachusetts Institute of Technology was supported by the National Science Foundation (NSF); the present research is supported by U.S. Army Tech Base funding at the U.S. Army Materials Technology Laboratory (Watertown, MA), and by the NSF at Northwestern University.

*Present address: Metals Research Branch, U.S. Army Materials Technology Laboratory, Watertown, MA 02172.

†Present address: Department of Materials Science and Engineering, Northwestern University, Evanston, IL 60208.

[1]G. B. Olson and M. Cohen, in *Dislocations in Solids,* edited by F. R. N. Nabarro, (North-Holland, Amsterdam, 1986), Vol. 7, pp. 297–407; G. B. Olson, in *Proceedings of the International Conference on Martensitic Transformations* (ICOMAT-86) (Japan Institute of Metals, Miyagi, 1987), pp. 25–34.

[2]A. L. Roitburd, in *Solid State Physics,* edited by F. Seitz, D. Turnbull, and H. Ehrenreich (Academic, New York, 1978), Vol. 32, p. 317; A. L. Roitburd, Usp. Fiz. Nauk. **113**, 69 (1974) [Sov. Phys.—Usp. **17**, 326 (1974)].

[3]Z. Nishiyama, *Martensitic Transformations* (Academic, New York, 1978).

[4]E. C. Bain, Trans. Am. Inst. Min. Metall. Pet. Eng. **70**, 25 (1924).

[5]Y.-Y. Ye, Y. Chen, K.-M. Ho, B. N. Harmon, and P. A. Lingård, Phys. Rev. Lett. **58**, 1769 (1987); Y. Chen, K.-M. Ho, and B. N. Harmon, Phys. Rev. B **37**, 283 (1988); these papers investigate two-strain paths of martensitic transformations in Zr and Ba using the frozen-phonon method.

[6]A. L. Roitburd, in *Phase Transformations 87,* edited by G. W. Lorimer (Institute of Metals, London, 1988), p. 414.

[7]G. L. Krasko and G. B. Olson (unpublished).

[8]T. Suzuki and H. M. Ledbetter, Philos. Mag. A **48**, 83 (1983); M. J. Kelly, J. Phys. F **9**, 1921 (1979); P. Beauchamp and J. P. Villain, in *Proceedings of the International Conference on Solid-Solid Phase Transformations,* edited by A. Aaronson (TMS-AIME, Warrendale, PA, 1982), p. 1221; J. Watton, Ph.D. thesis, Massachusetts Institute of Technology, 1983.

[9]V. L. Moruzzi, J. F. Janak, and A. R. Williams, *Calculated Electronic Properties of Metals* (Pergamon, New York, 1978).

[10]K. B. Hathaway, H. J. F. Jansen, and A. J. Freeman, Phys. Rev. B **31**, 7603 (1985).

[11]V. L. Moruzzi, Phys. Rev. Lett. **57**, 2211 (1986).

[12]V. L. Moruzzi, P. M. Marcus, K. Schwarz, and P. Mohn, Phys. Rev. B **34**, 1784 (1986).

[13]H. J. F. Jansen and S. S. Peng, Phys. Rev. B **37**, 2689 (1988).

[14]E. C. Stoner, Proc. R. Soc. London, Ser. A **169**, 339 (1939).

[15]O. K. Andersen, O. Jepsen, and D. Gloetzel, in *Highlights of Condensed Matter Theory,* edited by F. Bassani, F. Fumi, and M. P. Tosi (North-Holland, New York, 1985); O. K. Andersen, in *Electronic Structure of Complex Systems,* edited by P. Phariseau and W. M. Timmerman (Plenum, New York, 1984), pp. 11–65; H. L. Skriver, *The LMTO Method* (Springer, Berlin, 1984).

[16]D. Gloetzel and O. K. Andersen (unpublished); N. E. Christensen, Phys. Rev. B **32**, 207 (1985); H. L. Skriver, Phys. Rev. B **31**, 1909 (1985).

[17]U. von Barth and L. Hedin, J. Phys. C **5**, 1629 (1972).

[18]U. von Barth and C. D. Gelatt, Jr., Phys. Rev. B **21**, 2222 (1980).

[19]O. K. Andersen, J. Madsen, U. K. Paulsen, O. Jepsen, and J. Kollar, Physica B+C **86-88B**, 249 (1977).

[20]S. H. Vosko and P. Perdew, Can. J. Phys. **53**, 1385 (1975).
[21]O. Gunnarsson, J. Phys. F **6**, 587 (1976).
[22]J. F. Janak, Phys. Rev. B **16**, 255 (1977).
[23]U. K. Poulsen, J. Kollar, and O. K. Andersen, J. Phys. F **6**, L241 (1976); D. M. Roy and D. G. Pettifor, J. Phys. F **7**, 1183 (1977).
[24]G. L. Krasko, Phys. Rev. B **36**, 8565 (1987).
[25]The recently developed so-called "fixed-spin-moment" method in fact enables one to perform a more comprehensive analysis of magnetic behavior than the traditional spin-polarized calculations. For a detailed study of ferromagnetism and magnetic phase transformations in transition metals see Refs. 11, 12, and 26-28.
[26]V. L. Moruzzi, P. M. Marcus, and P. C. Pattnaik, Phys. Rev. B **37**, 8003 (1988).
[27]V. L. Moruzzi and P. M. Marcus, Phys. Rev. B **38**, 1613 (1988).
[28]P. M. Marcus and V. L. Moruzzi, Phys. Rev. B **38**, 6949 (1988).
[29]Recently (Ref. 28), the Stoner model has been generalized to allow for dependence of I on $\mathbf{m}$. A term quadratic in $\mathbf{m}$ was included, and the corresponding coefficient found using the fixed-spin-moment procedure Ref. 25.
[30]G. L. Krasko, Solid State Commun. **70**, 1099 (1989).
[31]The value $\beta=1.080$ would make an even closer fit of s_0. However, we decided to do all the calculations with $\beta=1.075$, since this is the same value that was used in Ref. 24 for the analysis of metamagnetism of fcc iron.
[32]Such a dependence on Ω generates the equation of state of the Murnaghan-Burch type: F. D. Murnaghan, *Finite Deformation of an Elastic Solid* (Wiley, New York, 1951); F. Birch, J. Geophys. Res. **57**, 227 (1952).
[33]L. Kaufman and H. Bernstein, *Computer Calculations of Phase Diagrams* (Academic, New York, 1970).
[34]W. P. Pearson, *Handbook of Lattice Spacings and Structures of Metals and Alloys* (Pergamon, Oxford, 1964).
[35]*Landolt-Börnstein,* New Series, edited by K. H. Hellwege (Springer-Verlag, Berlin, 1984), Vol. 18, Table 1.2.1, p. 10.
[36]W. Bendick and W. Pepperhoff, Acta Metall. **30**, 679 (1982).
[37]No calculations for $s<2.5$ a.u. were made because the frozen-core approximation would give a significant error at high densities. However, the linear extrapolation of the $IN(E_F)$ plot for the bcc phase shows that at $s\leq 2.33$ the NM phase does exist. The analysis of the behavior of the function $W_d(s)\overline{N(m,s)}$ [where $W_d(s)$ is the d-band width], which is almost independent of s, at $m=0$ shows that at $s=2.33$ a second-order phase transition into the FM state should occur (see Fig. 8, case $\alpha<0$, of Ref. 24). In fact, the fixed-spin-moment calculations show (Ref. 26) that at $s<2.28$ the NM bcc is stable, and at $s=2.28$ a second-order phase transition occurs, stabilizing the FM phase.
[38]J. Hubbard, Phys. Rev. B **19**, 2626 (1979); **20**, 4584 (1979).
[39]P. W. Bridgman, as quoted in R. Andersen, J. Phys. Chem. Solids, **27**, 547 (1966).
[40]R. L. Clendenen and H. G. Drickamer, J. Phys. Chem. Solids, **25**, 865 (1964).
[41]P. M. Giles, M. H. Longenbach, and A. R. Marder, J. Appl. Phys. **42**, 4290 (1971).
[42]I. A. Morrison, M. H. Kang, and E. J. Mell, Phys. Rev. B **39**, 1575 (1989).
[43]K. G. Tauer and R. J. Weiss, Bull. Am. Phys. Soc. **6**, 125 (1961); L. Kaufman, E. V. Clougherty, and R. J. Weiss, Acta Metall. **11**, 323 (1963); R. J. Weiss, Proc. R. Soc. London **82**, 281 (1963).
[44]C. Abrahams, L. Guttman, and J. S. Kasper, Phys. Rev. **127**, 2052 (1962); G. Johnson, M. B. McGirr, and D. A. Wheeler, Phys. Rev. B **1**, 3208 (1970).
[45]U. Gonser, R. Krischel, and S. Nasu, J. Magn. Magn. Mater. **15-18**, 1145 (1980).
[46]J. G. Wright, Philos. Mag. **24**, 217 (1971); U. Gradmann, W. Kümmerle, and P. Tillmanns, Thin Solid Films, **34**, 249 (1976); R. F. Willis, J. A. C. Bland, and W. Schwarzacher, J. Appl. Phys. **63**, 4051 (1988).
[47]N. E. Christensen (private communication).
[48]L. Delaey, P. F. Gobin, G. Guenin, and H. Warlimont, in *Proceedings of the International Conference on Martensitic Transformations* (ICOMAT-79) (Massachusetts Institute of Technology, Cambridge, MA, 1979), p. 400.
[49]G. B. Olson and M. Cohen, in *Proceedings of the International Conference on Solid-Solid Phase Transformations,* edited by H. I. Aaronson (TMS-AIME, Warrendale, PA, 1982), p. 1145.
[50]B. Olson and M. Cohen, in *Proceedings of the International Conference on Martensitic Transformations* (ICOMAT-82) [J. Phys. (Paris) Colloq. **43**, C4-75 (1982)].
[51]G. B. Olson, in *Proceedings of the International Conference on Martensitic Transformations* (ICOMAT-86) (Japan Institute of Metals, Miyagi, 1987), p. 25.